Cerebral Microbleed Detection by Extracting Area and Number from Susceptibility Weighted Imagery Using Convolutional Neural Network

IOP Conf. Series: Journal of Physics: Conf. Series **1229** (2019) 012038 doi:10.1088/1742-6596/1229/1/012038

Cerebral Microbleed Detection by Extracting Area and Number from Susceptibility Weighted Imagery Using Convolutional Neural Network

S Sa-ngiem[1, a], K Dittakan[1, b], K Temkiatvises[2, c], S Yaisoongnern[2, d] and K Kespechara[2, e]

[1] College of Computing, Prince of Songkla University Phuket Campus. 80 M.1 Vishit-songkram Road, Kathu, Phuket 83120, Thailand
[2] Bangkok Hospital, Phuket 83000, Thailand.

[a]bourson6@gmail.com; [b]kwankamon.d@psu.ac.th; [c]kanya.te@bgh.co.th; [d]Sirisak.ya@bgh.co.th; [e]kongkiatk@gmail.com

Abstract Cerebral microbleed (CMB) the small vessels in the brain which is one of the major factors used to facilitate in the early stage diagnosis for Alzheimer's disease detection. In traditional, CMBs detection can be done manually by the neurologists, doctors or specialists. However, the process is time-consuming and the results are not accurate depending on the doctor experiences. Therefore the efficient and reliable of the automatic detection of CMB is needed. This paper proposes a new framework for CMB detection which employs segmentation of the region of interests (ROIs), detection of the CMBs and identification of the area from SWI scan images. Convolutional Neural Network(CNN) is applied to generate the desired models for later prediction. Shape matching mechanism is also applied to identify locations of CMB in the brain. The experimental result shows that the CMB can be classified with a recorded accuracy value of 95.45%. The CMBs were discovered from three different locations include (i) cortical region, (ii) cerebellum and (iii) brainstem with an accuracy value of 100%.

1. Introduction

The brain is an organ that is the centre of the human nervous system. Cerebral Microbleed (CMB) is a small long-standing brain haemorrhage. The cause of the CMB is unclear but from many works of literature hypertension and cerebral ischemia are the factors concerned with CMB [1]. A possible long-term reaction of CMB is the Alzheimer's disease. Thus CMB is used as one of the factors in the Alzheimer's disease detection.

In order to detect CMB Magnetic resonance imaging (MRI) technologies is suggested. More specifically the Susceptibility Weighted Imaging (SWI) brain scan is considered as the main evidence in CMB identification. In general, CMB has a spherical shape and has a diameter of *2-10* mm [2]. However, there are some objects give a similar shape to CMB, such as macro-bleed, calcification, iron deposit, and deoxyhaemoglobin. The macro-bleed has a diameter of *5-10* mm, the size is bigger when compared to CMB [3]. The calcifications and iron deposit have a smaller focus point and lower intensity. The area found deoxyhaemoglobin is different from the area where the CMB is found [4]. From the literature reported that *19-83*% of patients with stroke are also found the CMBs. While *15-35*% of the patients with ischemic stroke are also found the CMBs [5]. Patients with CMB have a chance to face problems with daily activities such as speaking, walking and remembering. In traditional, CMB is

identified by neurologists using MRI image. However, the process has two main disadvantages: (i) difficult to complete in the short time, and (ii) the results are uncertain depending on the expert experiences.

The solution proposed in this work is based on the fundamental ideas of detecting the ROIs using various techniques of image processing. A collection of ROIs is used to generate the desire classifiers which can be applied to predict the classes (refers to CMB and non-CMB) of the unseen image in the future. Once the classifiers have been generated and then the areas of the detected CMBs are then extracted. The challenges of this work are: (i) duplicated CMB because the size of CMB is between 2 mm – 10 mm, so one CMB might be detected in multiple SWI images, and (ii) difficulty to detect because some CMB shapes are not completely in the circular shape. In the context of the work presented in this paper, the proposed framework offers the advantages on spending shorter time to diagnosis.

This paper is separated into eight sections and organised as follows. Section 2 describes an overview of some related works. The proposed framework of CMB detection by extracting area and number from Susceptibility Weighted Imagery (SWI) using CNN is presented in Section 3. The detail of region of interest detection used in this work is introduced in Section 4. The classifier generation mechanism, typically a brief description of CNN is given in Section 5. The overview of the CMB location extraction is then described in Section 6. Section 7 presents the experiments and the obtained results of the proposed framework. The conclusions, discussion and some future works are discussed in Section 8.

2. Related work

Medical imaging is the source of clinical evidence which is used to obtain the internal organs structure. The image helps the doctor in the diagnosis process. Medical imaging is a simple process to generate. The process provides a low effect on the patient body. In general, the medical images have been used in the hospital. There are various types of medical images have been discovered. The examples include: (i) X-ray, (ii) Computed Tomography, (iii) Magnetic Resonance Imaging, (iv) Positron Emission Tomography, and (v) Ultrasound.

The medical imaging is also applied to the human brain in the process of diagnosis of symptoms and disease conditions. A brain is a part of the central nervous system (CNR). The brain is located in the head which is the centre of the CNR. The brain controls body activities such as movement, behaviours, heartbeat, blood pressure, temperature, balance liquid in the body, cognition, motor learning, temper, and memory. The brain consists of three main different areas: (i) forebrain, (ii) midbrain, and (iii) hindbrain. The largest part in the brain is cerebrum (part of the forebrain). The cerebrum controls muscle, speaking, seeing, smelling, and testing.

There are many works have been proposed for automatic CMB detection using medical images. Seghier et al. proposed the automated segmentation and mixtures of Gaussians techniques in CMB detection [6]. Barnes et al. presented a semi-automatic method to identify CMB from other hyperintensities in SWI using the support vector machine (SVM) [7]. Bian et al. reported the process of CMB detection using a 2D fast radial symmetry transform (RST) method to locate potential CMB candidates [8]. Then the geometric feature examination was applied to remove false positives (FPs). Fazlollahi et al. utilized a novel cascade of random forest (RF) classifiers which trained from random transform based features to detect the CMBs [9]. Hao Chen et al. presented an automatic method using deep learning based 3D feature representation [10].

The main limitation of these previous works that it could be detected only shape, size, and compactness. Therefore in the context of this work, a framework of automated CMB detection and CMB area extraction from SWI brain scan is proposed.

3. Proposed Framework

The proposed framework of CMB detection by extracting area and number from SWI using the convolutional neural network is described in this section. A schematic of the proposed framework is given in Figure 1. The framework encompasses of two major phases: (a) classifier generation, and (b) CMB detection.

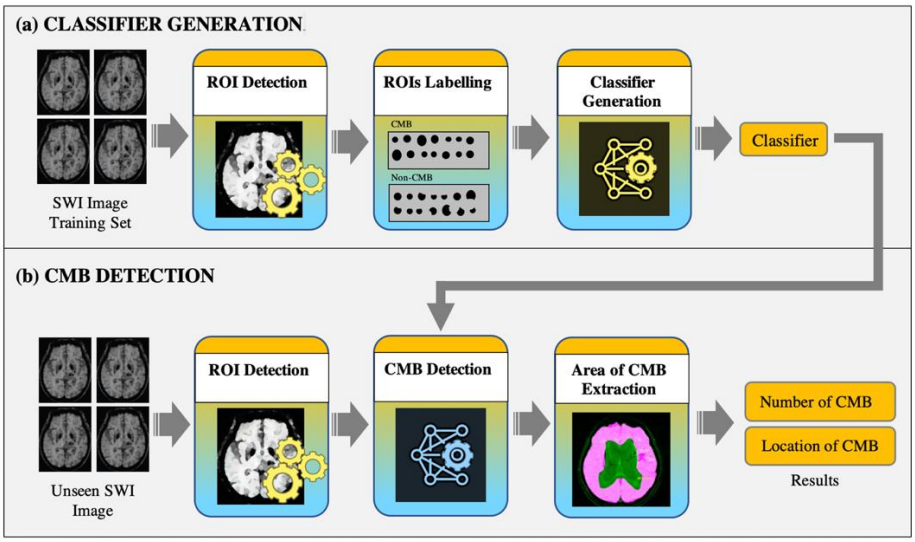

Figure 1. Proposed CMB detection from SWI image framework.

The classifier generation is the first phase of the proposed framework (the top half of Figure 1). The major aim of this phase is the desired classifiers construction. The generated classifiers can be used to predict the data class of unseen SWI images in the second phase. The classifier generation is a three-processes phase as shown in Figure 1(a). The figure shows that this phase consists of three processes: (i) region of interest (ROI) identification, (ii) ROIs labelling, and (iii) classifier generation. This phase starts with a collection of SWI images (called as a training data set). The initiating process is the ROI identification. The training SWI image is enhanced and transformed the original image into the proper image so that the region of interest (ROI) can be obtained. The full detail of the ROI identification process is presented in Section 4. Once the ROI identification process is completed, the acquired ROIs is manually labelled by the neurologists or the experts before the classifier generation process could be commenced. A collection of ROIs together with their class labels (refer to CMB or Non-CMB) is used in the classifier generation process. In order to construct the classifiers, the machine learning mechanism is then performed. More specifically, with respect to the work presented in this paper the convolutional neural network (CNN) is then applied. The brief description of CNN used in this work is given in Section 5. Once the classifier generation process is completed and the classifiers (prediction models) have been generated could be later applied to identify the CMBs from unseen SWI image in the second phase.

The second part of the overall framework (see the bottom half of Figure 1) is concerned with prediction model usage. This phase consists of three individual processes: (i) ROI identification, (ii) CMB detection, (iii) Area of CMB extraction. The process prior to the CMB could be detected from the unseen SWI image is ROI identification. In this phase, the ROI is identified using the same manner process as the ROI identification mentioned in the first phase (see above). A generated prediction model (from the first phase) is then applied to a collection of obtained ROIs in order to detect the CMBs. When an isolate CMB is detected, the next process is to extract the location or the area in the brain corresponding to given CMB.

4. ROI Detection

This section describes the region of interest (ROI) detection processes applied to the SWI input image. In order to identify the expected areas that might be the CMBs is the main purpose of the process, the process is given in Figure 2. An example of SWI image acquired from a patient is illustrated in Figure 2(a). However, prior ROI detection could be applied it was first necessary to enhance the quality of the images so that each the intensity of each SWI image was adjusted by spatial filtering smoothing method and boost filtering method. The result is presented in Figure 2(b). Once the image intensity was enhanced, the image was then converted each greyscale colour space into the binary colour image so that the brain

of SWI image can be clearly seen. The result is shown in Figure 2(c). However, the binary image may contain some noises and holes. Thus the morphological reconstruction method was then applied to eliminate the noises and fill the holes. The resulting image is given in Figure 2(d) so that the brain area can be clearly isolated. Once the brain area has been identified so that the image was used as the image mask. The mask was used to segment the brain from original image from Figure 2(a), the skull free image is presented in Figure 2(f).

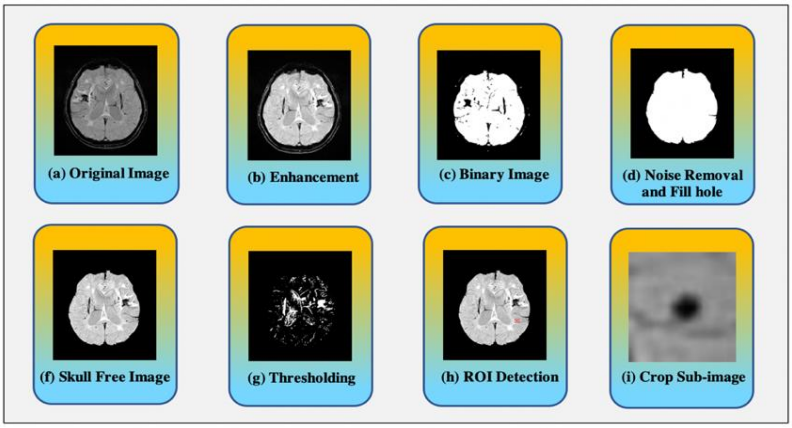

Figure 2. Region of Interest (ROI) Identification Process

In order to identify the ROIs from segmented image, the thresholding mechanism was applied. With respect to this work, three different values of threshold were used: (i) threshold = 80, (ii) threshold = 140, and (iii) threshold = 180. When each threshold value was adopted, the example result image (as the thresholding image) is presented in Figure 2(g). There were various parameters were examined whether the area met the conditions or not: (i) Size, (ii) Eccentricity, and (iii) Roundness. The first condition, a size of an area was evaluated. As noticed before the size of CMBs is between 2 mm to 10 mm (*7- 35 pixels*). Thus if the size of identified area was not met the condition, it was eliminated. Once the identified area has been measured, the second condition the eccentricity of an eclipse was then carried out. The eccentricity of the oval shape is a measurement ratio of the distance between the centre and the focus of an ellipse to its semi-transverse axis. The result of the eccentricity is a number of the range between *'0'* and *'1'*. If the shape is a circle, the eccentricity value is zero. While if the shape is a squashed ellipse, the eccentricity value is one. In the context of this work, the value of eccentricity less than *0.75* was used. Again if the identified area was not meet the condition (eccentricity greater or equal to *0.75*), the area was removed.

After the eccentricity of identified area has been computed, the roundness of the area was then calculated. The roundness is the measurement that the shape is close to a mathematically perfect circle or not. The result of the roundness is a number of the range between *'0'* and *'1'*. In case of roundness is one, the shape is a circle. On the other hand the roundness is zero, the shape is a squashed ellipse. According to this work roundness value of greater or equal to 0.8 was suggested.

Once the isolated area was examined with all three conditions (size, eccentricity, and roundness) described above, so that this area was defined as the ROI. The example results of ROI detection is shown in Figure 2(h). Finally, the identified ROI was then cropped into the size of '*36 x 36'* pixels as illustrated in Figure2(i).

5. Convolutional Neural Network

This section is described the fundamental idea of the Convolutional Neural Network refers to CNN or *ConvNet*. CNN is a class of deep learning and commonly used to analyse an image includes image recognition, image classification, and video labelling. The examples application using the CNN are: real-time voice activities detection on smart phone [11], gastric cancer detection from endoscopic images [12], and land uses classification from high resolution remote sensing images [13].

The CNN structure is comprised of three different layers: (i) convolutional layer, (ii) pooling layer, and (iii) fully-connected layer. The convolutional layer is comprised of a set of the learnable kernels. The objective of this layer is to extract local features from the input images. According to this work, the input image is a collection of segmented sub-images of ROIs. Each kernel is used to generate a feature map. The feature map units are applied to connect a small area of an input image. Once the feature maps are generated. To reduce the resolution of the previous feature maps, the pooling is then applied. Pooling splits the inputs into the disjoint areas in order to produce one output from each area. Fully connected layer connects all units in one layer to every unit in another layer. Four different of CNN methods were applied in the context of this research: (i) *AlexNet* [12], (ii) *GoogleNet*, (iii) *RestNet50*, and (iv) *SqueezeNet* [14,15,16]

6. Area Extraction

Once the CMBs areas were detected using the generated classifiers (the classifier was generated using the process as presented in the classifier generation phase). After that, the area of each identified CMB was then extracted. The area of CMB extraction process is given in this section. The process starts with the brain image together with the detected CMBs. In order to extract the locations of the detected CMB, the shape matching mechanism was suggested. Shape matching is the process of matching a target binary image to a collection of known shapes. With respect to this work, there are three different areas in the brain were extracted: (i) cortical region, (ii) cerebellum, and (iii) brainstem.

7. Evaluation

The evaluation of the proposed CMB detection framework is presented in this section. The evaluation was conducted using the data obtained from the local hospital in Phuket, Thailand. The further detail of the data set used for the context of this work is provided in Sub-section 7.1. Sub-section 7.2 reports a set of experiments to identify the most appropriate classification models for future CMB detection. Finally, Sub-section 7.3 presents the results obtained from applying the proposed mechanism in the context of a testing data set.

7.1. Data Set

For the evaluation, a total of *1,338* SWI images were collected from *26* cases. The data set was separated into two categories: (i) a set of *818* the SWI images from *16* cases were used as the training data set; and (ii) a set of *520* the SWI images from *10* cases as the testing data set. All image data sets were obtained from the local hospital in Phuket, Thailand. The image used in this work was represented in greyscale using the DICOM (Digital Image and Communication on medicine) format for SWI images. In general, the thickness of the SWI image is *3* mm. Thus there were *40-60* images obtained for each patient. The SWI images were taken using a transverse plane.

7.2. Classifier Generation

In order to identify the effect on classification performance on various generated classifiers is described in this sub-section. A training image data set of *818* SWI images from16 patients was used according to classifier generation purposes. A total *13,554* ROIs was obtained using the ROI detection process mentioned before in Section 4. The class label of an isolated area was given by the specialists and the neurologists. The *1,125* areas were labelled as CMB and *12,429* areas were labelled as non-CMB.

Once the *13,779* sub-images were segmented, the sub-images were then converted into three different forms: (i) original sub-image refers to '*Dataset 1*', (ii) resized sub-image to '*28 x 28'* pixels refers to '*Dataset 2'*, and (iii) only ROI sub-image refers to '*Dataset 3'*. Recall that four CNN mechanisms (see detail in Section 5) were considered: (i) *AlexNet*, (ii) *GoogleNet*, (iii) *ResNet50*, and (iv) *SqueezeNet*. In the context of classification performance evaluation, the five different numbers of the sample were also evaluated (*1,000, 2,000, 3,000, 4,000*, and *5,000 samples*). The classification performances were recorded in term of an accuracy using 80% of sample was the training.

The results obtained from the *Dataset 1* on four different CNN methods are given in Figure 3. From the figure, it can be concluded that with respect to the *Dataset 1*, the AlexNet method using *5,000* samples produced the best result with the accuracy value of 96.27%. In the context of the *Dataset 2*, the results from the experiments are shown in Figure 4. The main findings from the Figure 5 are the *GoogleNet* obtained the best classification result with the accuracy value of 95.96% when trained with *5000* samples. Finally, the results the experiments obtained from the *Dataset 3* are given in Figure 5. From the figure, it shows that the *GoogleNet* obtained the best performance result with the accuracy value of 94.45% using the training data set of *5000* samples.

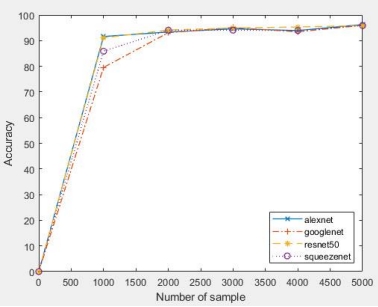

Figure 3. Dataset 1 results

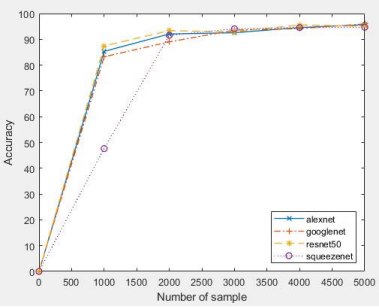

Figure 4. Dataset 2 results

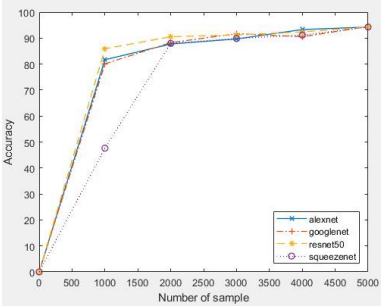

Figure 5. Dataset 3 results

The main findings of this sub-section can be concluded that: (i) the dataset 1 was the most appropriate data set used in classifier generation process because the *dataset 1* was the original greyscale sub-image encapsulated more information needed for classifier construction; (ii) the *AlexNet* mechanism was suggested in order to generate the classifier with high performance and reasonable processing time when compared to other methods; and (iii) more data sample was more accurate as presented of all data sets.

7.3. CMB Detection

Once the models have been generated using the CNN methods (see Section 5). Recall to the evaluations from the previous sub-section, the model generated from the *AlexNet* using 5000 samples with the dataset 1 produced the best classification performance. This section presents the obtained classifier usages. The test image data set was obtained from 512 SWI image collected from 10 patients. The results from the second phase from the framework presented in Figure 1 were: (i) 21 from 22 CMBs were detected from the generated classifier, and (ii) the areas of detected 21 CMBs were 100% accrete (15 CMBs in cortical region, 5 CMBs in cerebellum, and 1 CMB in brainstem).

8. Conclusions

The novel mechanism for the cerebral microbleed (CMB) detection from the susceptibility weighted imaging (SWI) images using the convolutional neural network (CNN). The objectives are to identify the CMBs and extract the area from the particular CMBs. The main findings from the work were: (i) the *AlexNet* and the ResNet50 techniques produced the high classification performances (see full detail in Section 5), (ii) dataset 1 was the subimage obtained from the process in Section 4 produced the best results on classification performance, and (iii) three different areas were extracted (refer to (i) cortical region, (ii) cerebellum, and (iii) brainstem) using the proposed area extraction process (the detail was discussed in Section 6).

However, in the future work, more CNN techniques may be carried out and the larger training data sets should be conducted.

Acknowledgments

We would like to thank Bangkok Hospital Phuket for providing us with the image data used for evaluation purposes with respect to the work presented in this paper.

References

[1] Noorbakhsh-Sabet N, Pulakanti V C and Zand R 2017 Uncommon Causes of Cerebral Microbleeds Journal of Stroke and Cerebrovascular Diseases 26 2043-49
[2] Gregoire S M, Werring D J, Chaudhary U J, Thornton J S, Brown M M, Yousry T A, and Jäger H R 2010 Choice of echo time on GRE T2*-weighted MRI influences the classification of brain microbleeds Clinical radiology 65 391-4
[3] Greenberg S M, Vernooij M W, Cordonnier C, Viswanathan A, Salman R A S, Warach S, and Microbleed Study Group 2009 Cerebral microbleeds: a guide to detection and interpretation The Lancet Neurology 8 165-174
[4] Maini R and Aggarwal H 2010 A comprehensive review of image enhancement techniques arXiv preprint arXiv:1003.4053
[5] Senthilkumaran N and Vaithegi S 2016 Image segmentation by using thresholding techniques for medical images Computer Science & Engineering: An International Journal 6 1-13
[6] Seghier M L, Kolanko M A, Leff A P, Jäger H R, Gregoire S M and Werring D J 2011 Microbleed detection using automated segmentation (MIDAS): a new method applicable to standard clinical MR images PloS one 6 e17547
[7] Barnes S R, Haacke E M, Ayaz M, Boikov A S, Kirsch W and Kido D 2011 Semiautomated detection of cerebral microbleeds in magnetic resonance images Magnetic resonance imaging 29 844-852
[8] Bian W, Hess C P, Chang S M, Nelson S J, and Lupo J M 2013 Computer-aided detection of radiation-induced cerebral microbleeds on susceptibility-weighted MR images NeuroImage: clinical 2 282-290
[9] Fazlollahi A, Meriaudeau F, Villemagne V L, Rowe C C, Yates P, Salvado O, and Bourgeat P 2014 April Efficient machine learning framework for computer-aided detection of cerebral microbleeds using the radon transform Biomedical Imaging (ISBI), 2014 IEEE 11th International Symposium 113-6
[10] Chen H, Yu L, Dou Q, Shi L, Mok V C and Heng P A 2015 April Automatic detection of cerebral microbleeds via deep learning based 3d feature representation Biomedical Imaging (ISBI), 2015 IEEE 12th International Symposium 764-7
[11] Li G and Yu Y 2016 Visual saliency detection based on multiscale deep CNN features IEEE Transactions on Image Processing 25 5012-24
[12] Krizhevsky A, Sutskever I and Hinton G E 2012 Imagenet classification with deep convolutional neural networks Advances in neural information processing systems 1097-1105
[13] Szegedy C, Vanhoucke V, Ioffe S, Shlens J and Wojna Z 2016 Rethinking the inception architecture for computer vision Proceedings of the IEEE conference on computer vision and pattern recognition 2818-26
[14] Han X, Zhong Y, Cao L and Zhang L 2017 Pre-trained AlexNet architecture with pyramid pooling and supervision for high spatial resolution remote sensing image scene classification Remote Sensing 9 848
[15] He K, Zhang X, Ren S and Sun J 2016 Deep residual learning for image recognition Proceedings of the IEEE conference on computer vision and pattern recognition 770-8
[16] Iandola F N, Han S, Moskewicz M W, Ashraf K, Dally W J and Keutzer K 2016 Squeezenet: Alexnet-level accuracy with 50x fewer parameters and< 0.5 mb model size arXiv (preprint arXiv:1602.07360)